ARCHIVES OF ELECTRICAL ENGINEERING VOL. 68(4), pp. 843–858 (2019)

DOI 10.24425/aee.2019.130687

Research on torque ripple suppression of brushless DC motor based on PWM modulation

ZHANG DAODE, LINGKANG WEI, XINYU HU, CHUPENG ZHANG, XUESHENG LI

School of Mechanical Engineering
Hubei University of Technology, China
e-mail: zhangdaode012@yeah.net

(Received: 15.03.2019, revised: 18.06.2019)

Abstract: Brushless DC motors are often used as the power sources for modern ship electric propulsion systems. Due to the electromagnetic torque ripple of the motor, the traditional control method reduces the drive performance of the motor under load changes. Aiming at the problem of the torque ripple of the DC brushless motor during a non-commutation period, this paper analysis the reasons for the torque ripple caused by pulse-width modulation (PWM), and proposes a PWM_ON_PWM method to suppress the torque ripple of the DC brushless motor. Based on the mathematical model of a DC brushless motor, this method adopts a double closed-loop control method based on fuzzy control to suppress the torque ripple of the DC brushless motor. The fuzzy control technology is integrated into the parameter tuning process of the proportional–integral–derivative (PID) controller to effectively improve the stability of the motor control system. Under the Matlab/Simulink platform, the response performance of different PID control methods and the torque characteristics of different PWM modulation methods are simulated and compared. The results show that the fuzzy adaptive PID control method has good dynamic response performance. It is verified that the PWM_ON_PWM modulation method can effectively suppress the torque ripple of the motor during non-commutation period, improve the stability of the double closed-loop control system and meet the driving performance of the motor under different load conditions.

Key words: DC brushless motor, electric propulsion, fuzzy PID control, torque ripple, PWM_ON_PWM modulation

1. Introduction

A modern ship electric propulsion system requires high power density and reliability. A brushless DC motor (BLDCM) is widely used in the field of electric drive because of its good speed regulation performance, high power density, high average torque and simple control strategy, so

it is very suitable to use the brushless DC motor as power source [1]. Torque characteristic is an important index of the motor performance, but the torque ripple in the BLDCM operation limits its application in high precision occasions. Therefore, the suppression of torque ripple and the improvement of control performance become the key to improve the performance of the BLDCM system [2].

Literature [3, 4] has carried out a simple analysis of the effects of different PWM methods on torque ripple during non-commutation, but no feasible solution has been proposed. Literature [5] gives the law of the occurrence of the off-phase current in different PWM modes. Literature [6] first presents the problem of suppression of torque ripple during non-commutation by PWM_ON_PWM, but it is not used for further quantitative analysis. The control method adopted in reference [7] can only suppress the torque ripple of the permanent magnet brushless DC motor running in the low speed region. Therefore, it is necessary to study the methods to suppress the torque ripple of a permanent magnet brushless DC motor in high speed region. Reference [8] suppresses the torque ripple generated by the commutation by the commutation overlap method. Literature [9] deeply analyzes the particularity of the direct torque control technology of a brushless DC motor. In [10], it is analyzed that the PWM_ON_PWM mode can completely suppress the torque ripple caused by the non-conduction phase current during non-commutation. Based on the previous research, this paper integrates the fuzzy control technology into the PID controller parameter tuning process, and analyzes and verifies that the PWM_ON_PWM n mode has a good suppression effect on the torque ripple during non-commutation.

2. Mathematical model and control strategy of brushless DC motor

2.1. Working principle and mathematical model of brushless DC motor

A brushless DC motor has evolved from the traditional brushless DC motor. The stator armature windings are star-connected and rotate in the three-phase six-state mode. The driving mode is a state in a three-phase bridge controlled inverter circuit. The rotor position is obtained by a Hall position sensor. The obtained rotor position can be processed as commutation control information, and the signal is passed through the driving circuit. To provide the switching signal for a power transistor, complete motor commutation and rotation. Fig. 1 is the working principle block diagram of a brushless DC motor [11].

In order to simplify the analysis, the following assumptions are made for the motor: without considering the core saturation, eddy current loss and hysteresis loss; without considering armature reaction, the air gap magnetic field is a trapezoidal wave with a flat top width of 120 degrees; without considering the alveolar effect; the power tube and the continuous current diode of the inverting circuit have ideal switching characteristics [12, 13].

According to the equivalent circuit, the three-phase winding phase voltage equation of the motor can be expressed as [14]:

$$\begin{bmatrix} u_{AN} \\ u_{BN} \\ u_{CN} \end{bmatrix} = \begin{bmatrix} R & 0 & 0 \\ 0 & R & 0 \\ 0 & 0 & R \end{bmatrix} \begin{bmatrix} i_A \\ i_B \\ i_C \end{bmatrix} + \begin{bmatrix} L_S & M & M \\ M & L_S & M \\ M & M & L_S \end{bmatrix} \frac{\mathrm{d}}{\mathrm{d}t} \begin{bmatrix} i_A \\ i_B \\ i_C \end{bmatrix} + \begin{bmatrix} e_A \\ e_B \\ e_C \end{bmatrix}, \tag{1}$$

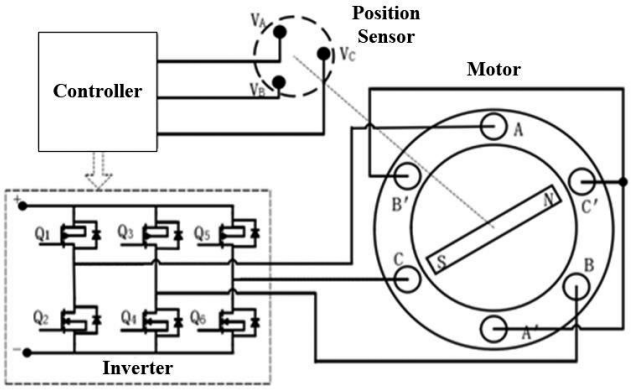

Fig. 1. Working principle of brushless DC motor

u_{AN}, u_{BN}, u_{CN} represent the three-phase voltage, i_A, i_B, i_C represent the three-phase current, e_A, e_B, e_C represent the three-phase electromotive force, R is the stator phase resistance, L_S is the three-phase winding self-inductance, M is the mutual inductance between two-phase windings.

The three-phase current of star winding is satisfied:

$$i_A + i_B + i_C = 0. \tag{2}$$

The voltage equation of the brushless DC motor is as follows:

$$\begin{bmatrix} u_{AN} \\ u_{BN} \\ u_{CN} \end{bmatrix} = \begin{bmatrix} R & 0 & 0 \\ 0 & R & 0 \\ 0 & 0 & R \end{bmatrix} \begin{bmatrix} i_A \\ i_B \\ i_C \end{bmatrix} + \begin{bmatrix} L & 0 & 0 \\ 0 & L & 0 \\ 0 & 0 & L \end{bmatrix} \frac{\mathrm{d}}{\mathrm{d}t} \begin{bmatrix} i_A \\ i_B \\ i_C \end{bmatrix} + \begin{bmatrix} e_A \\ e_B \\ e_C \end{bmatrix}. \tag{3}$$

In the formula $L = L_S - M$.

The electromagnetic power of the motor is:

$$P_e = i_A e_A + i_B e_B + i_C e_C \,. \tag{4}$$

All the electromagnetic power is converted into the mechanical power of the mechanical load by the electromagnetic torque of the motor. Therefore, the electromagnetic torque of the motor is obtained as follows:

$$T_e = \frac{P_e}{\Omega}, \tag{5}$$

where Ω is the mechanical angular speed of the motor.

For brushless DC motors with two or two conducting modes, only two-phase windings generate torque at each time, and the phase current direction of the two-phase windings is opposite, and the direction of the back EMF is opposite, then the electromagnetic torque is simplified as follows:

$$T_e = \frac{2EI}{\Omega}, \tag{6}$$

I is the average amplitude of phase current, E is the reverse EMF amplitude.

The dynamic equation of the brushless DC motor is:

$$T_e = T_L + J\frac{\mathrm{d}\Omega}{\mathrm{d}t} + B\Omega, \tag{7}$$

T_L is the load torque, J is the rotating inertia of the system; T_L is the load torque, B is the viscous damping coefficient of the system.

2.2. Control strategy of DC brushless motor

A BLDCM is a time-varying and strongly coupled system. It is very important to select the appropriate control structure and algorithm to control and regulate the motor. The control structure is double closed-loop control, the inner loop is a current loop, and the outer loop is a speed loop. For the traditional PID algorithm it is difficult to eliminate the problem of system overshot and short-term oscillation in the control system of a brushless DC motor. This paper integrates the fuzzy control technology into the parameter setting process of the PID controller to better suppress the motor torque ripple and improve the stability of the control system. As shown in Fig. 2, it is a double closed-loop fuzzy control system diagram of a BLDCM. The current loop is controlled by PI and the speed loop is controlled by a fuzzy PID.

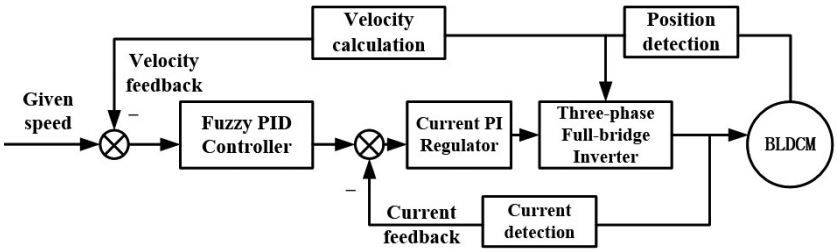

Fig. 2. Control system diagram of brushless DC motor

The self-adaptive fuzzy-PID controller is applied to the speed loop of a DC brushless motor, and a two-dimensional fuzzy controller is adopted. The speed error e and error rate $\dot{e}$ are taken as inputs, and the parameters of the PID are modified by using the fuzzy rules to meet the requirements of e and $\dot{e}$ at different times and self-tuning of the parameters of the PID. The structure of the controller is shown in Fig. 3.

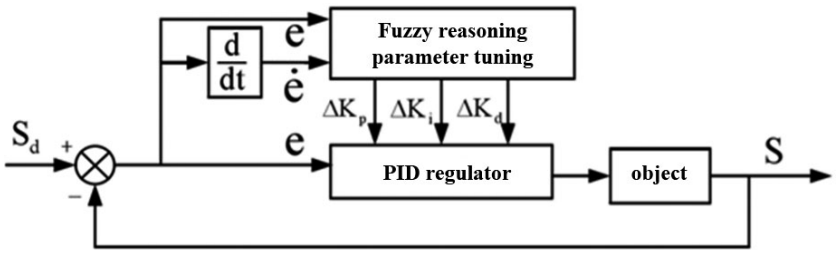

Fig. 3. Structure diagram of Fuzzy PID controller

According to the actual speed error of the BLDCM measured by a Hall sensor and expert experience, the basic domain of speed error of the fuzzy controller can be determined. For convenience of calculation, the basic domain is quantified by 0.5. The quantized domain is $\{6, -5, -4, -3, -2, -1, 0, 1, 2, 3, 4, 5, 6\}$ and the quantized factor of the deviation change rate is 100. The universe is $\{-6, -5, -4, -3, -2, -1, 0, 1, 2, 3, 4, 5, 6\}$.

The basic domains of proportional link coefficient K_P, integral link coefficient K_I and differential link coefficient K_D are $\{0.2, +0.2\}$, $\{0.1, +0.1\}$ and $\{0.1, +0.1\}$, respectively. The quantization factors are 30, 60 and 60, respectively. Therefore, the quantized domain is $\{6, -5, -4, -3, -2, -1, 0, 1, 2, 3, 4, 5, 6\}$.

According to the actual working characteristics of a brushless DC motor and expert experience, the rules of the speed fuzzy controller of the brushless DC motor are formulated. According to the fuzzy rule table, the output surface of three outputs of the controller is obtained. The smoother the surface, the more reasonable the fuzzy rule is established [11], as shown in Fig. 4.

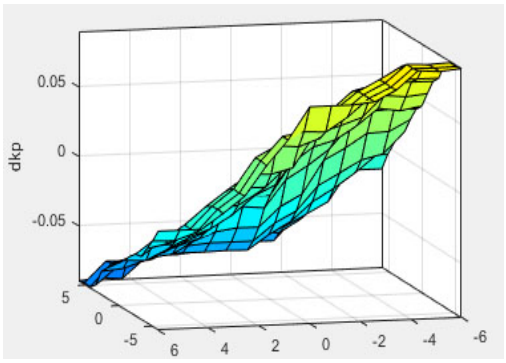

(a) Output curve of K_P

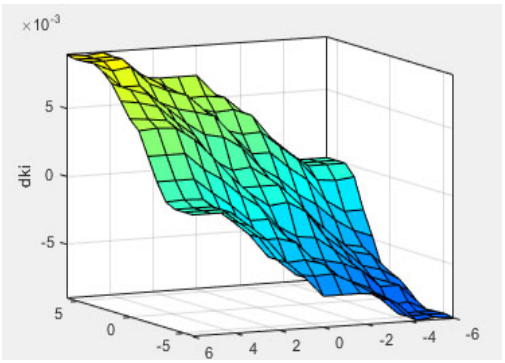

(b) Output curve of K_I

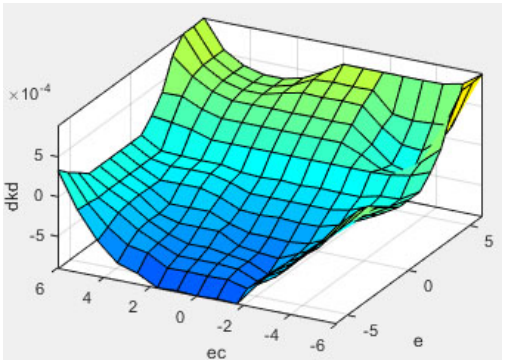

(c) Output curve of K_D

Fig. 4. Output curve

This section mainly introduces the working principle and mathematical model of a BLDCM, determines the control strategy of the BLDCM, and chooses the appropriate control structure and algorithm to control and regulate the motor. The control structure adopted is the double closed-

loop control. At the same time, the fuzzy control technology is integrated into the parameter setting process of the PID controller, and how to use the fuzzy controller to set the parameters is introduced, so as to better suppress the motor torque ripple and improve the stability of the control system.

3. Research on torque ripple reduction method based on PWM modulation

Although the double closed-loop fuzzy control system improves the control performance to a certain extent, it still cannot satisfy the motor in some occasions requiring higher accuracy, response speed and dynamic characteristics. This is because the control system does not introduce the control link to electromagnetic torque, which makes the motor have the problem of torque ripple. How to suppress the torque ripple is the key factor to improve the control performance of a brushless DC motor. This paper mainly analyses the non-commutation torque ripple of a brushless DC motor and its suppression methods, emphatically analyses the influence of different PWM modes on the torque ripple, and finally proposes the suppression analysis of the PWM_ON_PWM mode for the torque ripple.

3.1. The effect of PWM on torque ripple in non-commutation

There are two kinds of torque ripple in a BLDCM: a non-commutation period and commutation period. In this paper, the non-commutation torque ripple is studied. There are four common PWM modes for a brushless DC motor, namely H_PWM-L_ON, H_ON-L_PWM, PWM-ON and ON-PWM, as shown in Fig. 5.

For the condition of non-commutation torque ripple, the non-conducting phase voltage is U_{off} and the DC bus voltage is U_d. When $U_{off} < 0$, the four PWM modes generate non-conducting phase continuity through the lower arm diode, and when $U_{off} > U_d$, non-conducting phase continuity through the upper arm diode [15].

The following four common PWM modes are analyzed in each electrical angle range. As shown in Table 1, the non-commutation torque ripple values of different modulation modes in the

Table 1. Torque ripple values for different PWM modulation modes

PWM modulation modes	$0°\sim30°/60°\sim90°$	$30° sim 60°/90° sim 120°$
H_PWM-L_ON	$-\frac{2E^2}{L\Omega}t_1$	$-\frac{2E^2}{L\Omega}t_1-\frac{2e^2}{3L\Omega}t_1$
H_ON-L_PWM	$-\frac{2E^2}{L\Omega}t_1-\frac{2e^2}{3L\Omega}t_1$	$-\frac{2E^2}{L\Omega}t_1$
PWM-ON	$-\frac{2E^2}{L\Omega}t_1$	$-\frac{2E^2}{L\Omega}t_1-\frac{2e^2}{3L\Omega}t_1$
ON-PWM	$-\frac{2E^2}{L\Omega}t_1-\frac{2e^2}{3L\Omega}t_1$	$-\frac{2E^2}{L\Omega}t_1$

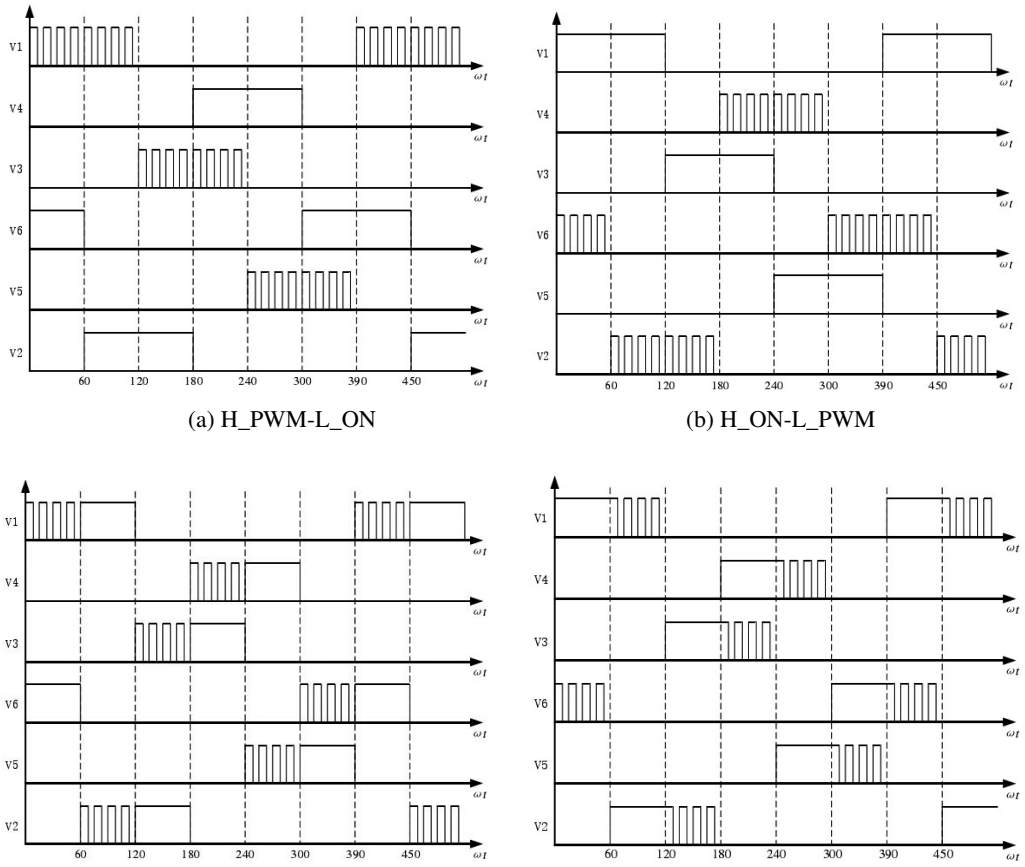

(a) H_PWM-L_ON (b) H_ON-L_PWM

(c) PWM-ON (d) ON-PWM

Fig. 5. Output curve

range of $0°sim120°$ are listed. The calculation results in the range of 120°~240° and 240°~360° are the same as 0°~120°.

As can be seen from Table 1:

1. Torque ripple ΔT produced by non-conducting phase continuation includes two parts: one is the torque ripple

$$\Delta T_1 = -\frac{2E^2}{L\Omega}t_1,$$

produced by off-phase continuation, the other is the increased part

$$\Delta T_2 = -\frac{2e^2}{3L\Omega}t_1.$$

This part of the torque ripple is not a fixed value, and the amplitude varies with the change of the non-conducting opposite electromotive force.

2. The amplitude of the torque ripple is also higher in the region where the absolute value of back EMF is larger; as the amplitude of the back EMF approaches zero, the torque ripple gradually decreases to zero. The off-phase discontinuous current is generated by a low-level PWM signal, so it is inevitable to turn off the phase discontinuous current when using two-two-on three-phase full-bridge topology.

From the above analysis, the four modulation methods are single-tube modulation, that is, only one of the power transistors performs PWM. However, these four PWM methods cause the non-conduction phase diode to continue to flow to generate torque ripple. When the PWM is turned off by the power transistor, the non-conducting phase voltage becomes greater than U_d or less than 0, then the diode conduction current occurs, which causes the torque ripple.

3.2. Torque pulse suppression method based on PWM_ON_PWM

From the previous analysis, it can be seen that the four PWM modes in common use cause non-conducting diode continuation in normal operation, which leads to the generation of torque ripple. In view of this situation, this paper uses PWM_ON_PWM to suppress the torque ripple, as shown in Fig. 6. In the 120 degree range of each power transistor conduction, the first 30 degrees and the last 30 degrees are PW modulated, and the middle 60 degrees are constant conduction [16–19].

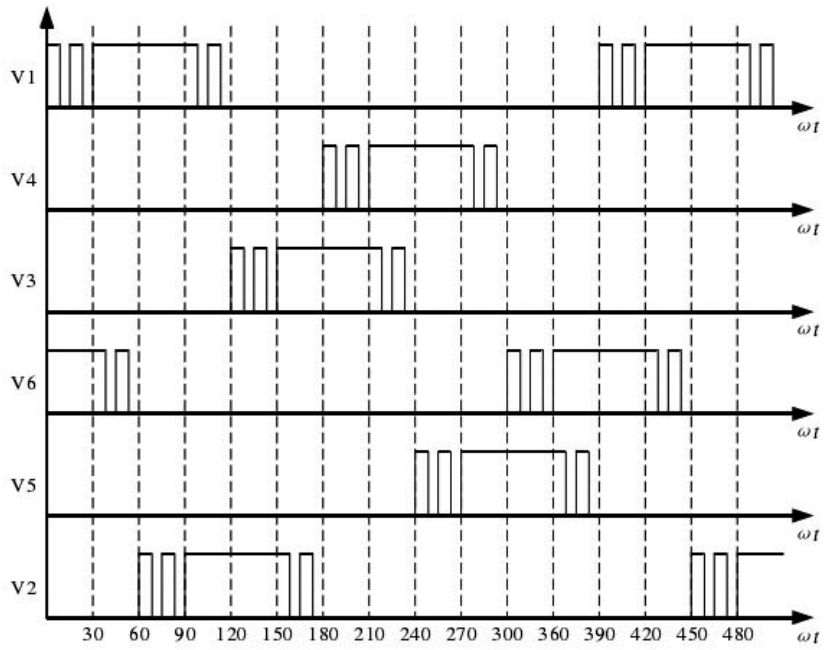

Fig. 6. PWM_ON_PWM modulation mode

The non-conducting phase voltage of PWM_ON_PWM mode satisfies $0 < U_{off} < U_d$ and only produces off-phase discontinuous current; the non-conducting phase voltage of PWM-ON,

ON-PWM, H_PWM-L_ON, H_ON-L_PWM mode will have three possibilities: $U_{off} < 0$, $U_{off} > U_d$ and $0 < U_{off} < U_d$, which will produce both an off-phase discontinuous current and a non-conducting phase discontinuous current [20]. Therefore, using PWM_ON_PWM can avoid the generation of non-conducting phase continuum flow.

The core of this modulation method is that when the non-conducting opposite electromotive force is greater than zero, the upper arm power transistor is PW modulated, and the lower arm power transistor is constant conduction. When the non-conducting opposite electromotive force is less than zero, the upper arm power transistor is constant conduction, and the lower arm power transistor is PW modulated. In this way, the non-conducting phase terminal voltage is neither higher than the DC bus voltage nor lower than zero, thus avoiding the phenomenon of non-conducting phase conduction. This modulation mode combines the advantages of half-bridge modulation and full-bridge modulation: it not only completely eliminates the phenomenon of non-conducting phase conduction, but also reduces the switching loss of power switches.

In order to minimize commutation torque ripple, feedback closed-loop control is adopted for non-commutation current, i.e. the real-time detection of non-commutation current. Through feedback control, the current can track the set current expectation in the real time, and then make the fluctuation of the non-commutation current smaller. Hysteresis current control is generally used for feedback closed-loop control.

As shown in Fig. 7, the principle of operation is that the current loop uses a *Schmitt hysteresis regulator*. By comparing the given current with the actual current, the output of the regulator is determined by the amplitude and hysteresis width of the actual current. When the actual current is less than the lower limit of the hysteresis width, the output of the controller is 1, and the corresponding power switch is on. When the current begins to rise to the upper limit of the hysteresis width, the output of the controller is 0, and the corresponding power switch is off and the current decreases. The characteristics of this method are good rapidity, simple application and good current limiting ability. Experiments show that the proposed method can suppress the commutation torque ripple effectively when the BLDCM runs in the middle and low speed regions [21].

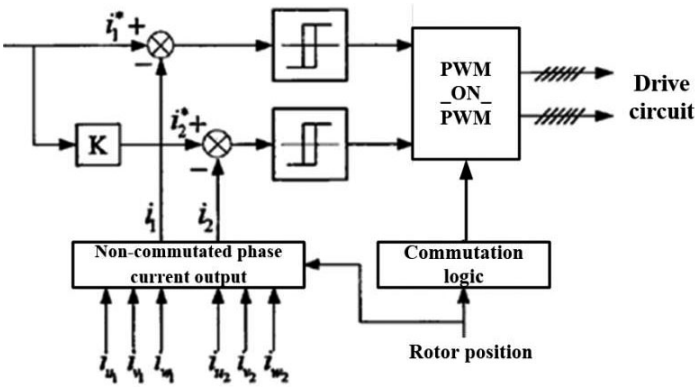

Fig. 7. Principle diagram of current hysteresis control

4. Simulation analysis of brushless DC motor control system

4.1. Simulation model of control system

According to the above analysis, the simulation model of the double closed-loop control system of a BLDCM is built based on the simulation platform of MATLAB/Simulink. According to the simulation model of the BLDCM, the parameters of the motor are as follows: stator resistance 0.9 Ω, stator inductance 0.27 mH, rotational inertia 4.8×10^{-5} kg·m^2, damping coefficient 0.001 N·m·s, pole number 4, as shown in Fig. 8.

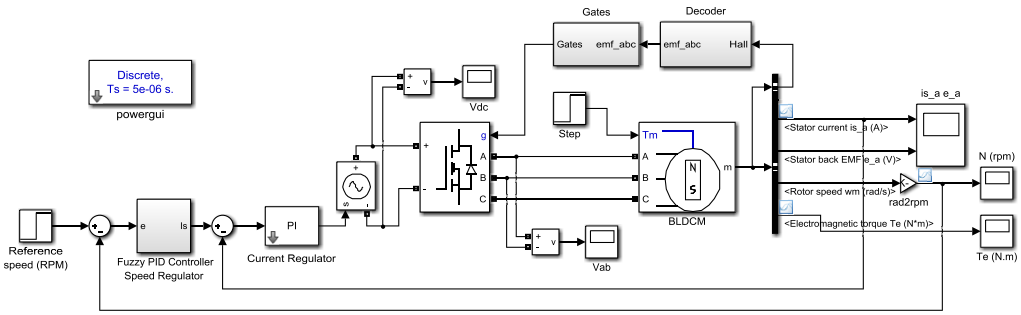

Fig. 8. Simulation model of brushless DC motor control system

In the simulation model of Matlab/Simulink, according to the control structure of the BLDCM, the whole system is divided into several modules: the BLDCM, Fuzzy PID speed control module (Fig. 9), current PI control module, inverting circuit module and logic commutation module.

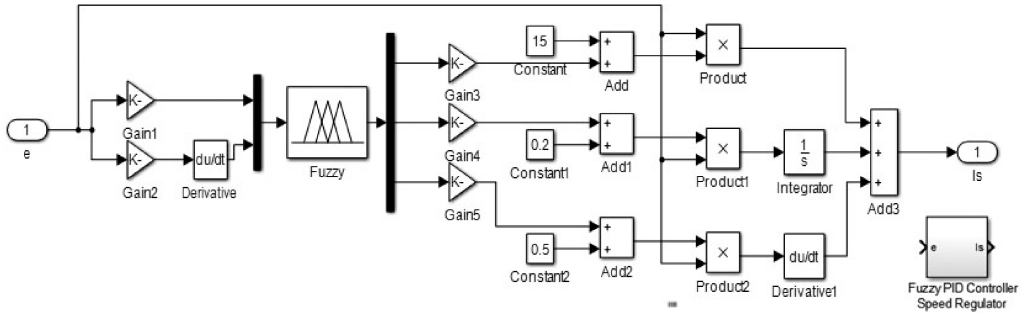

Fig. 9. Fuzzy PID controller speed regulator module

4.2. Analysis of simulation results

In this paper, the control system of a brushless DC motor is simulated and analyzed from two aspects: in order to verify the better response performance of the fuzzy PID control system to the control system, the response performance of the fuzzy PID control system and the traditional PID control system under the conditions of motor starting, load mutation and given speed mutation

is compared and analyzed; at the same time, in order to verify that the PWM_ON_PWM mode can effectively suppress the motor. Torque ripple, the effects of H_PWM-L_ON modulation and PWM_ON_PWM on motor torque ripple are compared and analyzed.

4.2.1. Comparison and analysis of different PID controls

As shown in Fig. 10, the speed response curves of a given motor speed of 2 000 rpm under no-load operation are controlled by Fuzzy PID and traditional PID.

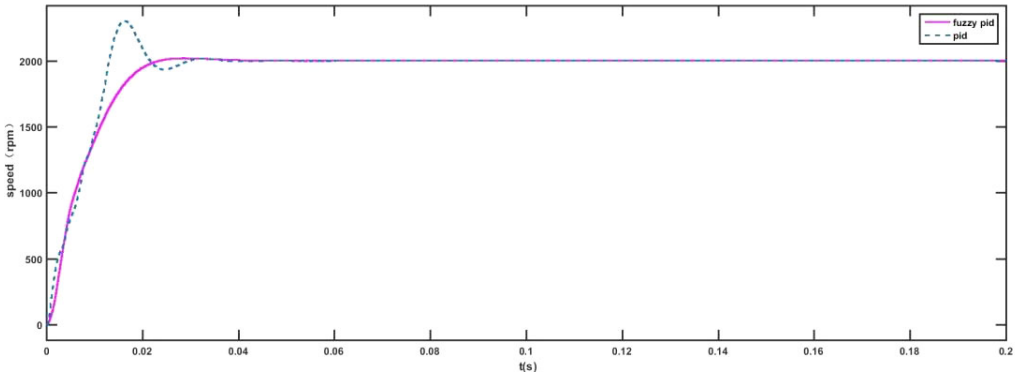

Fig. 10. No-load speed response diagram of 2 000 rpm motor speed

As shown in Fig. 11, given the starting speed of the motor is 1 000 rpm, the speed response curve of the motor, when it suddenly changes to 2 000 rpm at 0.1 s, is drawn.

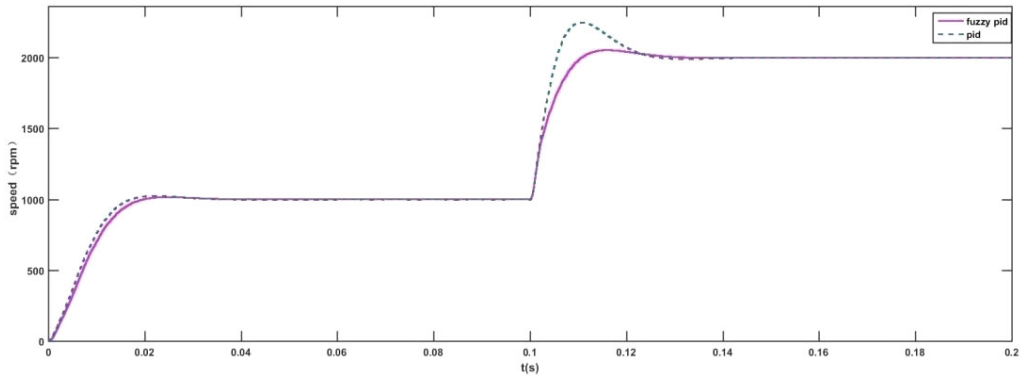

Fig. 11. Speed response diagram of sudden change of motor speed

As shown in Fig. 12, given a no-load operation speed of 2 000 rpm, the load changes from 0 N to 5 Nm at 0.1 s.

According to different given conditions, the simulation performance analysis tables of fuzzy PID and traditional PID control are arranged, as shown in Table 2.

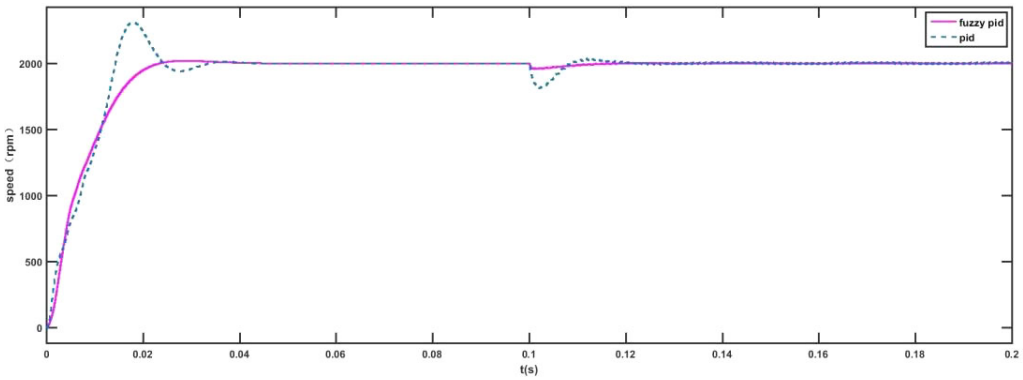

Fig. 12. Velocity response diagram of motor torque sudden change

Table 2. Analysis of system simulation performance

Speed/rpm	Fuzzy PID		PID	
	Overshoot (%)	Time (s)	Overshoot (%)	Time (s)
0–2 000 no load	0.8	0.038	15	0.042
1 000–2 000 no load	2	0.028	12	0.039
2 000 increase load	1.9	0.021	9	0.026

From the simulation results, it can be seen that under the given conditions, compared with the traditional PID control, the Fuzzy PID control has smaller overshoot and faster regulation speed. Under a no-load of 0–2 000 rpm, the traditional PID overshoot is 14.2% more than the Fuzzy PID overshoot; under a no-load of 0–2 000 rpm, the traditional PID overshoot is 10% more than the Fuzzy PID overshoot; under a sudden load of 2 000 rpm, the traditional PID overshoot is 7.1% more than the Fuzzy PID overshoot. Moreover, the adjustment speed of the Fuzzy PID control is faster. Therefore, the Fuzzy PID control has better and more stable response performance.

4.2.2. Comparison and analysis of different PWM modulation modes

As shown in Fig. 13(a–d), given a motor speed of 2 000 rpm, no-load start, in the case of 0.1 s sudden load of 5 Nm, electromagnetic torque waveform and phase current simulation waveform under two modulation modes.

Fig. 13(a–b) show that the torque fluctuation under PWM_ON_PWM mode is stable, and the amplitude is smaller, and the stable state can be achieved faster when the load changes abruptly.

Fig. 13(c–d) show that the phase current waveform of the motor under PWM_ON_PWM mode is more regular and the fluctuation is smaller, when the load changes abruptly, the fluctuation of current value is small, and it can quickly become stable.

The waveforms of phase currents under PWM_ON_PWM show that PWM_ON_PWM eliminates the problem of non-conducting phase continuum flow and thus eliminates the problem

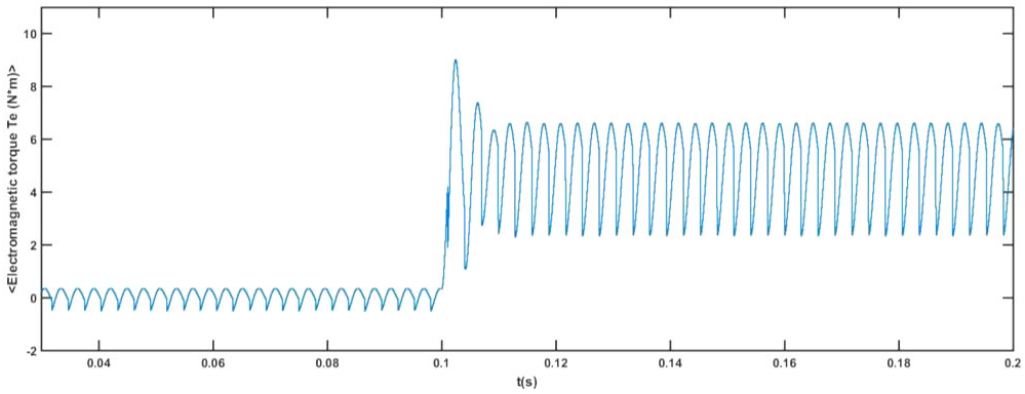

(a) H_PWM-L_ON modulation electromagnetic torque waveform

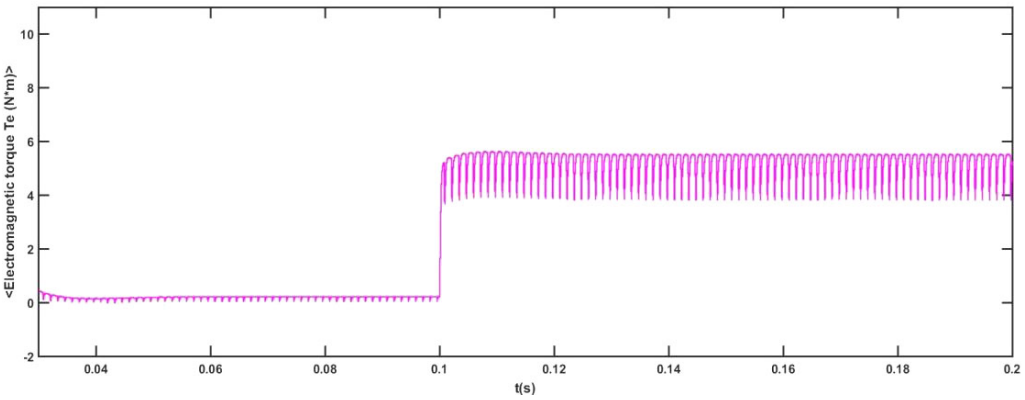

(b) PWM_ON_PWM electromagnetic torque waveform

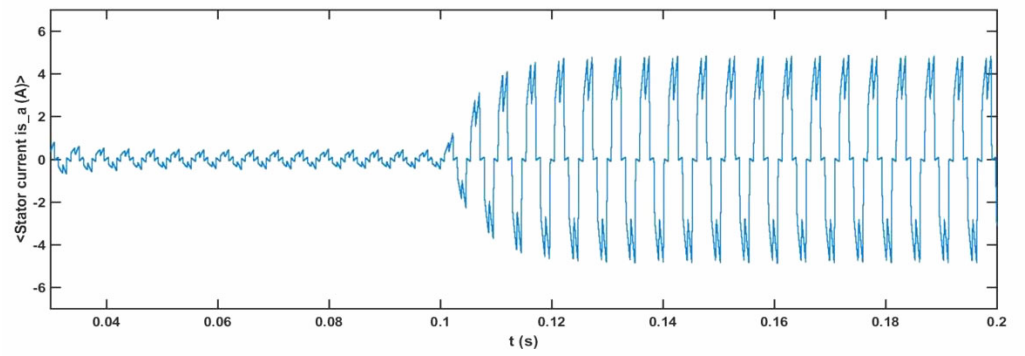

(c) H_PWM-L_ON modulation phase current waveform

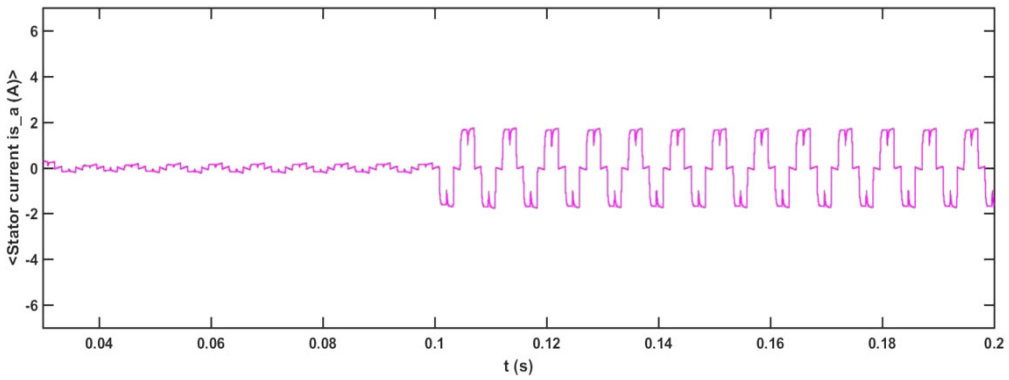

(d) PWM_ON_PWM phase current waveform

Fig. 13. Electromagnetic torque and phase current waveform of two modulation modes

of non-conducting phase torque ripple. When the H_PWM-L_ON modulation mode is applied at low speed and constant load, the current will form a loop in the winding through DC bus continuation, the amplitude of current drop will be larger, so we can see that the H_PWM-L_ON modulation mode has larger waveform amplitude than the PWM_ON_PWM mode. Therefore, it is verified that the PWM_ON_PWM can suppress the torque ripple of the motor well.

In this section, based on the simulation model of a BLDCM, the response performance of Fuzzy adaptive PID control and traditional PID and the influence of H_PWMŋL_ON and PWM_ON_PWM on torque ripple are compared and analyzed. Under the same speed and load conditions, the phase current waveform of PWM_ON_PWM mode is more regular and the fluctuation is smaller; under the same conditions, the PWM_ON_PWM mode can reach a stable state faster after a sudden load. The results show that the Fuzzy adaptive PID control has better response performance and the PWM_ON_PWM can better suppress the motor torque ripple.

5. Conclusion

This paper adopts a double closed loop control system, outer loop Fuzzy PID speed loop control, inner loop PID current loop control. Considering the influence of PWM on the torque ripple of a BLDCM, the PWM_ON_PWM is used to suppress the torque ripple of the BLDCM. The response performance of Fuzzy PID and traditional PID and the influence of H_PWMŋL_ON and PWM_ON_PWM on motor torque ripple are simulated and analyzed, respectively. The simulation results show that the Fuzzy PID has faster response, smaller overshoot and shorter adjustment time than traditional PID. The phase current waveform of PWM_ON_PWM is more regular and the torque ripple is smaller. It is verified that Fuzzy PID can improve the control performance of a DC brushless motor, and PWM_ON_PWM can effectively suppress the motor torque ripple.

Acknowledgements

This work is supported by the Wuhan science and technology support program (No. 201701020 1010137) and the National Natural Science Foundation of China (No. 61976083).

References

[1] Chen Liang, *Research on control technology of brushless DC motor for electric propulsion of warships*, Harbin University of Technology, vol. 18, no. 2, pp. 45–62 (2018).

[2] Zhang Yong, Cheng Xiaohua, *Research on Torque Ripple Suppression Measures for Brushless DC Motor*, Micromotor, vol. 46, no. 7, pp. 88–91 (2013).

[3] Zhou Jinghua, Jia Bin, Zhang Xiaowei, Li Zhengxi, *Dead-time compensation strategy for three-level inverters*, Journal of Motor and Control, vol. 54, no. 5, pp. 34–38 (2013).

[4] Luo Zhengqiang, Ding Wen, Yang Xintuan, Liang Deliang, *Mathematical model and characteristic analysis of dual redundancy permanent magnet brushless motor system*, Journal of Motor and Control, vol. 67, no. 3, pp. 55–57 (2013).

[5] Xue Xiaoming, Chen Hong, *Study on the open-phase current of brushless DC motor*, Journal of Electrical Technology, vol. 26, no. 4, pp. 64–70 (2011).

[6] Li Fengxiang, Zhu Weijin, *Research and application of dual-mode control technology for brushless DC motor*, Journal of Motor and Control, vol. 12, no. 3, pp. 57–59 (2013).

[7] Xu Jiafeng, *Research on control system of permanent magnet brushless DC motor*, Northeast University (2014).

[8] Xia Yonghong, Huang Shaogang, *Effect of excitation current pulsation on no-load voltage waveform of armature windings*, Journal of Motor and Control, vol. 25, no. 9, pp. 55–60 (2012).

[9] Zhang Lanhong, Tang Huiyu, He Jianqiang, *Direct Torque Control of Brushless DC Motor Based on Hall Position Signal*, Journal of Motor and Control, vol. 22, no. 9, pp. 56–63 (2018).

[10] Zhou Meilan, Li Zhi, Su Gehang, *The influence of PWM modulation mode of brushless DC motor on torque ripple during non-commutation period*, Journal of Harbin University of Technology, vol. 19, no. 6, pp. 74–81 (2014).

[11] Feng Jiapeng, *Design and research of DC brushless motor control system based on DSP*, South China University of Technology (2012).

[12] Pragasan Pillay, Krishnan R., *Modeling of permanent magnet motor drives*, IEEE Transactions on Industry Electronics, vol. 35, no. 4, pp. 537–541 (1988).

[13] Evans P.D., Brown D., *Simulation of brushless DC drives*, IEE Proceedings B, Electric Power Applications, vol. 137, no. 5, pp. 299–308 2001.

[14] Ruan Yi, Chen Weijun, *Motion Control System*, Tsinghua University Press, pp. 227–230 (2006).

[15] Chen Jian, Yu Shenbo, *Torque characteristics of PWM_ON_PWM modulation for brushless DC motor*, Journal of Motor and Control, vol. 20, no. 8, pp. 48–54+63 (2016).

[16] Anand Sathyan, Nikola Milivojevic, Young-Joo Lee, Mahesh Krishnamurthy, Ali Emadi, *An FPGA-Based Novel Digital PWM Control Scheme for BLDC Motor Drives*, IEEE Trans. Ind. Electron., vol. 56, no. 8, pp. 3040–3050, August (2009).

[17] Lin Y.K., Lai Y.S., *Pulse width modulation technique for BLDCM drives to reduce commutation torque ripple without calculation of commutation time*, IEEE Trans. Ind. Appl., vol. 47, no. 4, pp. 1786–1793, July/August (2011).

[18] Chen W., Liu Y., Li X., Shi T., Xia C.L., *A Novel Method of Reducing Commutation Torque Ripple for Brushless DC Motor Based on Cuk Converter*, IEEE Trans. Power Electron., vol. 32, no. 7, pp. 5497–5508, November (2017).

[19] Xia C.L., Jiang G.K., Chen W., Shi T.N., *Switching-Gain Adaption Current Control for Brushless DC Motors*, IEEE Trans. Ind. Electron., vol. 63, no. 4, pp. 2044–2052, April (2016).

[20] Pillay P., Krishnan R., *Modeling, simulation and analysis of permanent-magnet motor drives. II. The brushless DC motor drive*, IEEE Transactions on Industrial Electronics, vol. 25, no. 2, pp. 274–279 (1989).

[21] Huang Chaojie, *Research on control system of six-phase brushless DC motor*, Northeast University (2015).